Simulation of the Nevarro Target

J. D. Pecover, J. W. Skidmore, N.-P. L. Niasse, M. R. Betney, D. A. Chapman and N. A. Hawker
First Light Fusion Ltd., Unit 10 Oxford Industrial Park, Yarnton, OX5 1QU, United Kingdom
(Dated: April 19, 2022)

The Nevarro target has been successfully shot on First Light Fusion's large gas gun, resulting in detection of fusion neutrons. This report presents an overview of the neutron diagnostics from hydrodynamic simulation of the experiment, which resulted in a yield prediction of 39 neutrons, with lower and upper bounds of 19 and 43 neutrons respectively. In-depth probing of the burn weighted average (BWA) quantities of the plasma reveals that in the finest resolution simulation, neutrons are emitted from a region of plasma with average density 2500 $\mathrm{kg\,m^{-3}}$, ion temperature 240 eV and a volume equivalent to a sphere of radius 2.2 μm. The predicted neutron yield lies within the error bars of the experiment carried out on the BFG [1]. As the simulations do not contain any physical processes that can produce neutrons other than through thermonuclear fusion reactions, this is indicative that the experimentally observed neutrons are thermonuclear in origin.

Keywords: Nevarro target, B2, Richardson extrapolation, Grid Convergence Index, neutron yield

I. INTRODUCTION

A. Target Details

Nevarro is a novel uni-axially driven target developed by FLF which has been shot on the company's largest 2-stage light gas gun (BFG) (an explosively-driven launcher which accelerates solid, 15 mm radius heavy-metal tipped projectiles to velocities in excess of 6.5 $\mathrm{km\,s^{-1}}$), resulting in detection of fusion neutrons [1]. As Nevarro represents an important Trade Secret to the company, no further details of the target are provided at this time.

B. Hydrodynamics Code and Models

The present work is undertaken using 2D simulations carried out in B2, a 3D magneto-hydrodynamics code developed at FLF. Within the code, the hydrodynamics equations are solved on an Eulerian grid using a Lagrangian-remap technique in tandem with a volume-of-fluid [2] interface tracking algorithm. Also included is subcycled two-temperature thermal conduction and support for either analytic or tabulated models for material equations of state (EoS), plasma microphysics and fusion reactivity.

For the simulations in this report, material EoS tables were provided by the FEOS package [3], an extension of the QEOS model [4], with ionisation tables provided by the Thomas-Fermi model [5, 6]. Thermal conductivity tables for electrons and ions were generated using the Lee-More [7] and Stanton-Murillo [8] models respectively. The Lee-More model is corrected from the usual Lorentz approximation to include electron-electron scattering following the approach of Apfelbaum [9]. For the electron-ion energy exchange rate, the f-sum rule approach [10, 11] is employed, which has been shown to perform well compared to molecular dynamics simulations [12]. Further details of the physics models and configurations available can be found in [13].

II. SIMULATION METRICS AND TECHNIQUES

In this section, the calculation of neutron yield and useful associated metrics is described. There is also a brief summary of Richardson extrapolation and Grid Convergence Index, methods used in numerical analysis to estimate the actual value and associated error of a given quantity, using results from simulations at different resolutions.

A. Calculation of Neutron Yield

The volumetric neutron production rate (neutrons per $\mathrm{m^3}$ per second) for a deuterium plasma is given by:

$$Y_{\mathbf{r}t}(\mathbf{r},t) = \frac{1}{2} n_D^2 \langle \sigma v \rangle, \tag{1}$$

where n_D is the number of deuterium ions per cubic metre and $\langle \sigma v \rangle$ is the reactivity for the neutron-producing branch of the reaction, both of which in general vary in space and time. The reactivity has been parameterised as a function of temperature by Bosch and Hale [14], allowing the reactivity to be replaced with a function which calculates the reactivity based on an input temperature $g(T)$. To obtain the total neutron yield, Equation 1 must be integrated in space $\mathbf{r}$ and time t:

$$Y = \frac{1}{2} \int_0^{t_f} \mathrm{d}t \int_V \mathrm{d}\mathbf{r}\, n_D(\mathbf{r},t)^2 g(T(\mathbf{r},t)). \tag{2}$$

For each timestep in the hydrodynamics code, the neutron yield is calculated in each cell by calculating $Y(\mathbf{r},t)$ using the cell density and temperature, and multiplying the answer by the cell volume and timestep interval. Values in all cells are summed over all timesteps to give the total cumulative neutron yield at the end of the simulation.

B. Burn Weighted Average (BWA) quantities

The calculation of burn weighted average (BWA) quantities of the plasma provide useful zero-dimensional information about regions of the target plasma where neutrons are being emitted. Given a quantity $X(\mathbf{r}, t)$ which varies in space $\mathbf{r}$ and time t, the burn weighted average of X, $\langle X \rangle_b(t)$, as a function of time is given by:

$$\langle X \rangle_b(t) = \frac{\int_V Y_{\mathbf{r}t}(\mathbf{r}, t) X(\mathbf{r}, t) \mathrm{d}\mathbf{r}}{\int_V Y_{\mathbf{r}t}(\mathbf{r}, t) \mathrm{d}\mathbf{r}}. \tag{3}$$

In this report, the BWA density and ion temperature are chosen as metrics of interest.

C. Fusion Performance Averaged (FPA) quantities

When comparing simulations, it is often useful to extract single numbers from the time traces of the BWA quantities. One way to accomplish this is to take the BWA quantity at the point of maximum neutron production rate; this is, however, vulnerable to transient events that have a large neutron production rate but occur over a very short time period. An alternative method is, for each peak or 'event' in neutron production, to take the time-average of the BWA quantity over the peak, ie.

$$\langle X \rangle_{\text{event}} = \frac{1}{\tau_{\text{event}}} \int_{t_{\text{start}}}^{t_{\text{end}}} dt \langle X \rangle_b(t), \tag{4}$$

where the start and end times are determined by the full width at half maximum (FWHM) of the peak in neutron yield and τ_{event} is their difference (see [15] for discussion and detailed explanation of how these are calculated for simulations with multiple peaks). Average values of a BWA quantity over each event are then converted to fusion performance averaged (FPA) values by averaging all over peaks, weighted by the total neutron yield associated with each peak (Equation 13 in [15]); note that in this work all simulations contain only a single peak, meaning that the FPA values simplify to Equation 4. The FPA value of quantity X is denoted by $\langle X \rangle_{\text{f}}$.

D. Burn Volume

In addition to the raw neutron yield and BWA and FPA quantities, it is also interesting to estimate the volume over which the bulk of the yield occurs at a given time. This can be estimated from the total neutron production rate (ie. neutrons per second) and BWA or FPA quantities under the assumptions that:

- The yield for each timestep is dominated by regions with density and temperature close to the BWA or FPA values (almost certainly the case)
- The yield comes from a uniform volume at a density and temperature equal to the BWA or FPA values (more of an approximation)

A 'BWA' or 'FPA' volumetric neutron production rate can be determined from the BWA or FPA values though the use of Equation 1, where the deuterium number density is calculated from the appropriate density and the reactivity is calculated using the Bosch-Hale formulae with the appropriate ion temperature. Taking the ratio of the (instantaneous for BWA, averaged over the peak for FPA) total neutron production rate with this volumetric neutron production rate gives a burn volume, from which a burn radius r_b can be extracted under the assumption of a spherical fuel assembly. Note that using BWA values, which are time-dependent, gives a time-dependent burn radius $r_b(t)$; while using FPA values, which are averaged over time, give a time-averaged burn radius $\langle r_b \rangle_{\text{f}}$.

E. Richardson Extrapolation and Grid Convergence Index

Richardson extrapolation [16, 17] provides a mechanism for estimating the exact, 'zero-resolution' value and associated errors of a variable that is converging as resolution becomes finer over a series of numerical simulations. Consider a set of three hydrodynamics simulations at resolutions 1, 2 and 3 which give results for the variable f of f_1, f_2 and f_3, where 1 has the finest resolution and 3 has the coarsest: the Richardson extrapolation zero-resolution estimate for f, denoted f_0, is given by:

$$f_0 = f_1 + \frac{f_1 - f_2}{r^p - 1}, \tag{5}$$

where $r > 1$ is the ratio of resolutions and p is the order of convergence, which can be calculated using

$$p = \frac{\log\left(\frac{f_3 - f_2}{f_2 - f_1}\right)}{\log(r)}. \tag{6}$$

Under the assumption that a grid at infinitely high resolution will return the exact value of f_0, the error caused by use of finite grid resolution can be quantified using the grid convergence index (GCI) as defined by Roache [18]: this provides an estimate for the fractional error on f_1. The GCI for f evaluated on the finest grid (which has the value f_1), is defined as

$$\epsilon_{\text{GCI}} = \frac{F}{r^p - 1} \left| \frac{f_1 - f_2}{f_2} \right|, \tag{7}$$

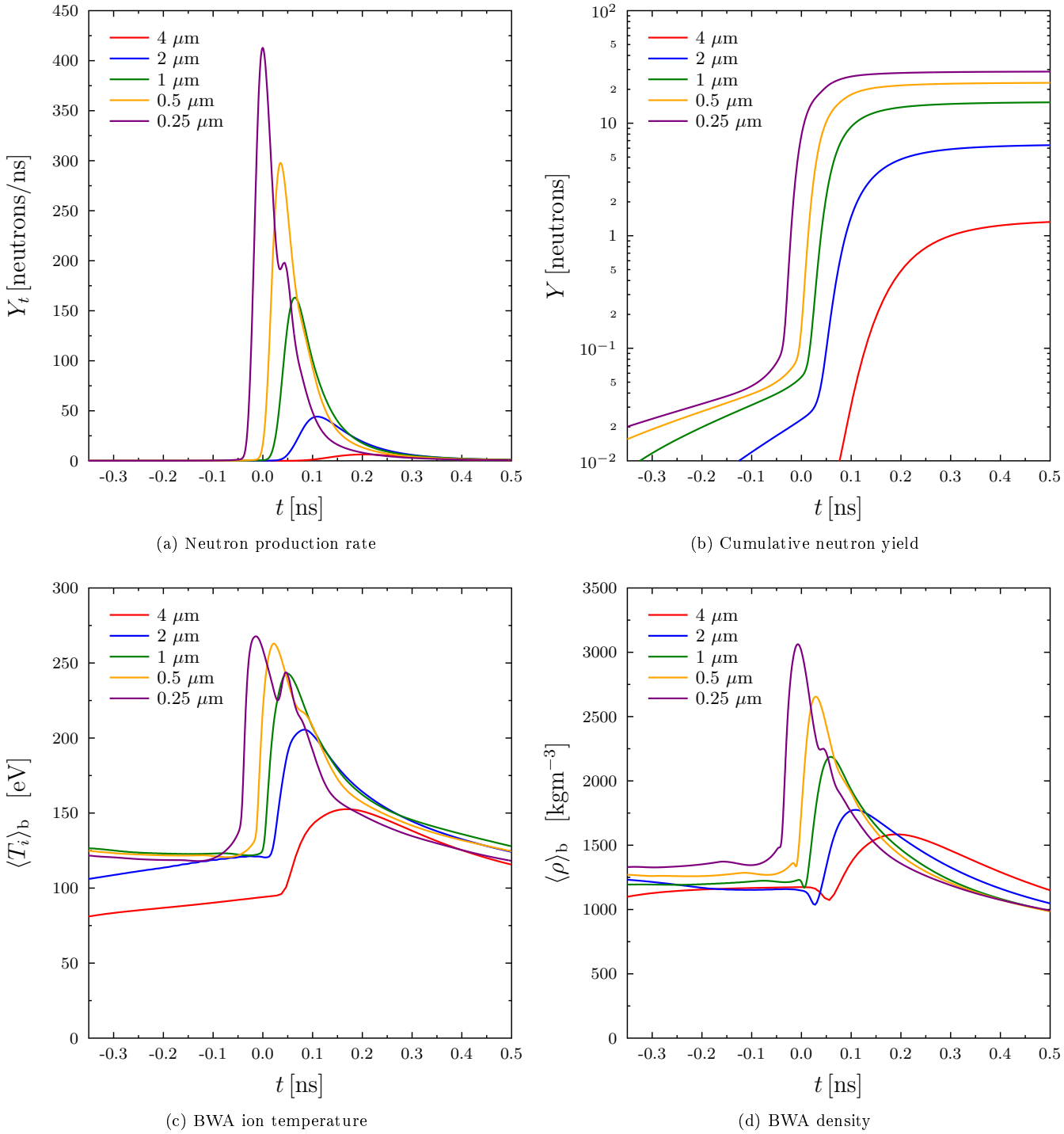

(a) Neutron production rate

(b) Cumulative neutron yield

(c) BWA ion temperature

(d) BWA density

Figure 1. **Simulation evolution in terms of neutron yield and BWA quantities.** Neutron production rate (a); cumulative neutron yield (b); BWA ion temperature (c) and BWA density (d) for B2 simulations with resolutions varying from 4 μm to 0.25 μm. As the resolution is increased, the burn pulse occurs progressively earlier and with a higher peak, and with higher peak BWA ion temperature and density. The burn width reduces to a point but appears to be converging. The cumulative neutron yield can also been seen to be converging, when plotted on a logarithmic axis.

where F is a safety factor. It has been found empirically that in order to give a 95% confidence that the true value lies within the error bounds, F should take the value 1.25 [18, 19]. The final value of the variable of interest on finest grid is then given by

$$f_1 \pm f_1 \epsilon_{\mathrm{GCI}}. \tag{8}$$

Note that this analysis considers only the uncertainty due to grid convergence; in reality there are many other uncertainties that are more difficult to quantify, such as those arising from settings in physical and numerical models within the code, and the impact of missing physics. This has been explored further (for different simulations) through sensitivity analyses carried out at FLF [13].

III. SIMULATION RESULTS

Nevarro was simulated using B2 at resolutions ranging from 8 μm to 0.25 μm; the finest resolution simulation produced a neutron yield of 29 neutrons with lower and upper bounds of 19 and 43 neutrons respectively; Richardson extrapolation suggests a 'zero resolution' neutron yield of 39 neutrons. The yield occurs in a plasma with an average density 2500 kg m^{-3}, ion temperature 240 eV and a volume equivalent to a sphere of radius 2.2 μm.

A. Grid Convergence

When carrying out hydrodynamics simulations, it is crucial to ensure that the resolution used is sufficient to resolve all physical processes of interest. In the case of fusion simulations, the most basic requirement is that the cumulative neutron yield converges to a constant value, providing a degree of confidence in the prediction of the simulation.

Figure 1 shows neutron production rate, cumulative neutron yield, BWA ion temperature and BWA density as functions of time for resolutions ranging from 4 μm to 0.25 μm (due to its low yield, the 8 μm resolution simulation was omitted). As the resolution is increased, the burn pulse occurs progressively earlier and with a higher, narrower peak, and with higher peak BWA ion temperature and density. The cumulative neutron yield, plotted on a logarithmic y-axis, increases and visibly converges with finer resolution. The BWA ion temperature and density both show a peak corresponding to peak neutron output, with smooth profiles suggesting that the neutron yield arises from a single region in the simulation.

A further increase in resolution beyond ~0.25 μm, in order to better estimate the cumulative neutron yield, is not possible due to the increasingly onerous computational requirements associated with such extreme resolu-

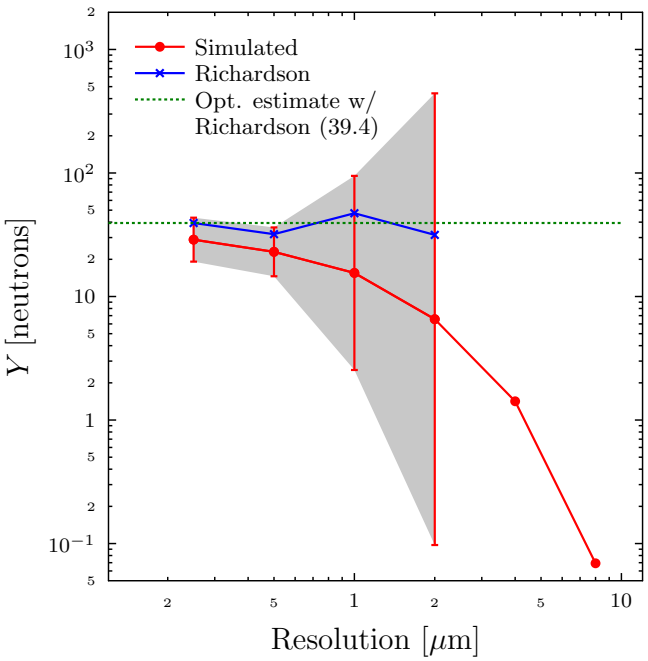

(a) Cumulative neutron yield on log-log axes

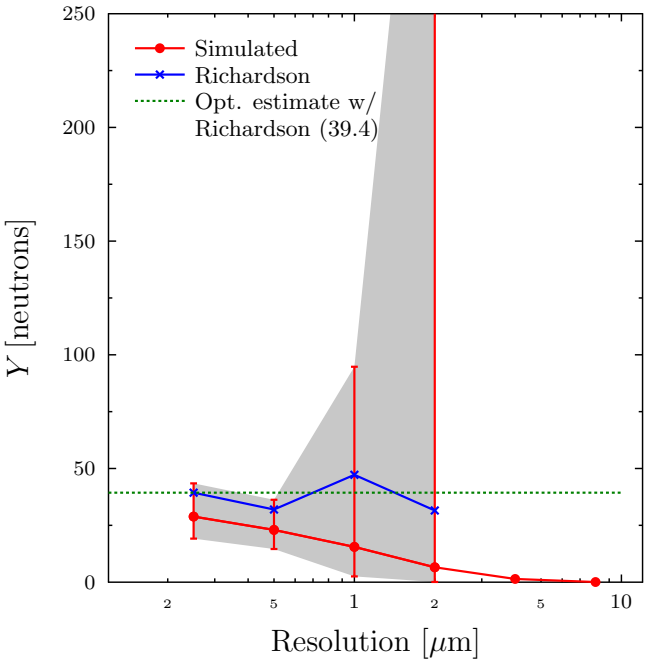

(b) Cumulative neutron yield on log-lin axes

Figure 2. **Neutron yield as a function of resolution, plotted on log-log axes (Figure 2a) and log-lin axes (Figure 2b).** The prediction from Richardson extrapolation is calculated using the neutron yield and that from the two next coarsest simulations in log space, giving a value at oscillates around ~ 40 neutrons. The best Richardson extrapolated value, between the finest and second-finest resolution, is plotted using a green dashed line and has the value 39 neutrons

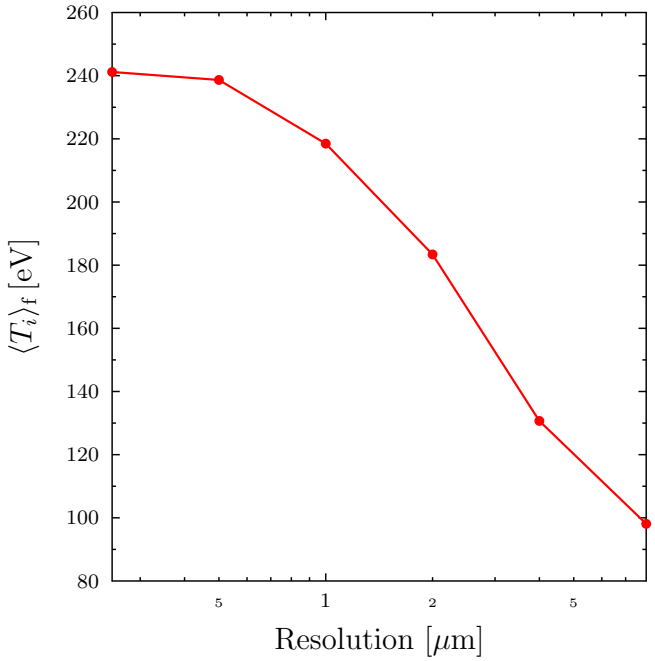

(a) FPA ion temperature (log-lin axes)

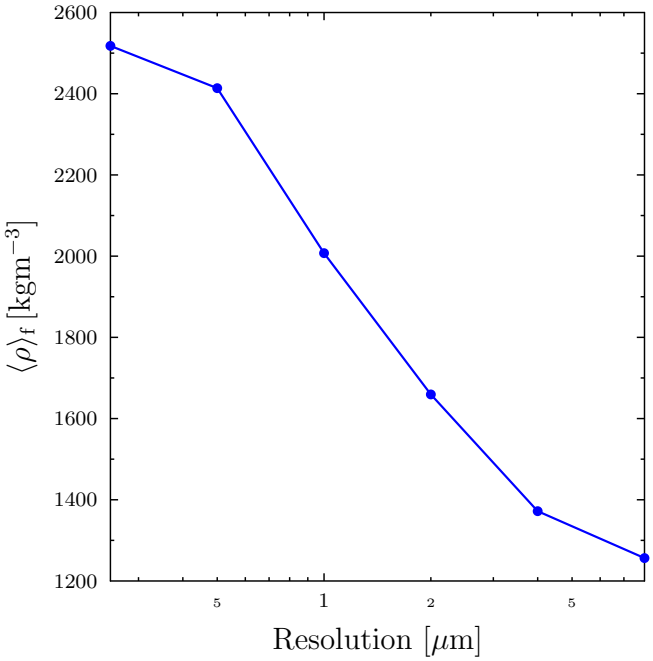

(b) FPA density (log-lin axes)

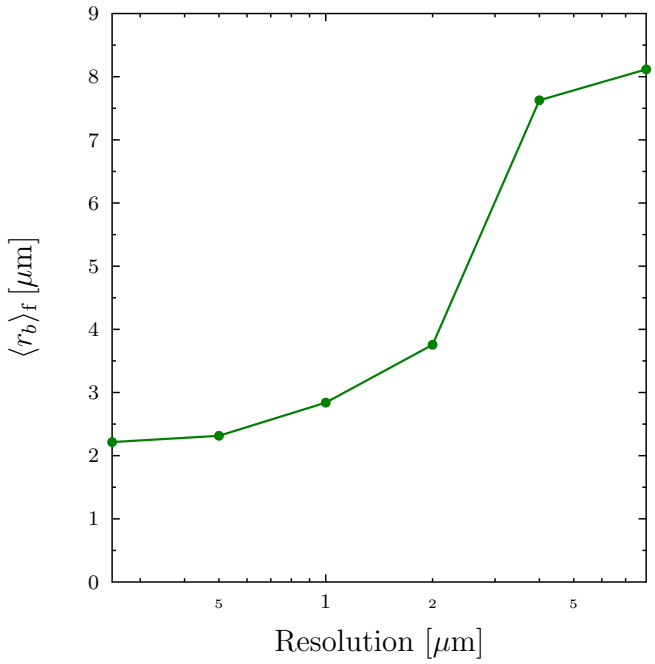

(c) FPA Spherical equivalent burn radius (log-lin axes)

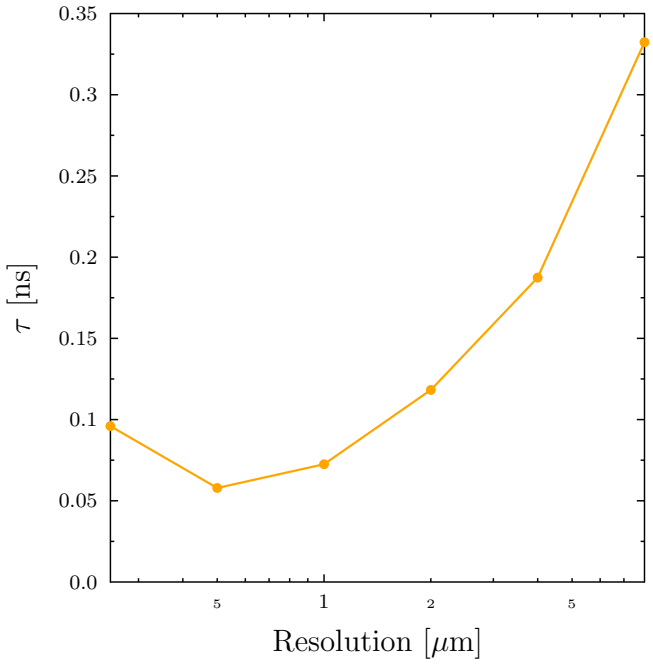

(d) Confinement time (log-lin axes)

Figure 3. **Resolution convergence of fusion performance average (FPA) quantities and confinement time.** Top row: density, ion temperature; bottom row: burn radius, confinement time. Density and ion temperature increase as the resolution becomes finer, with the FPA ion temperature clearly converging to ∼240 eV, with less clear convergence seen for the FPA density. Burn radius decreases as the resolution becomes finer, converging to ∼2.2 μm. The confinement time appears to be converging to ∼ 0.05 ns, but at the finest resolution increases to ∼0.1 ns. This can be explained by the splitting of the peak in neutron production rate in Figure 1a.

tion; it is possible, however, to obtain an improved answer using Richardson extrapolation (§II E). Due to the particular convergence characteristics of this simulation, optimal results were found by carrying out the extrapolation and GCI measurement using the logarithm of the neutron yield, then converting back to neutron yield by raising the extrapolated value and associated errors to the power of 10.

Results for cumulative neutron yield, with Richardson extrapolation and errors calculated using GCI, are shown in Figure 2, with log-log axes (Figure 2a) and log-lin axes (Figure 2b). At each resolution, the order of convergence (Equation 6) and prediction from Richardson extrapolation (Equation 5) are calculated using the neutron yield and that from the two next coarsest simulations in log space, meaning that for each simulation at or above 2 μm there is a prediction of the zero-resolution neutron yield – these are represented by the blue points on each panel and can be seen to oscillate around ~ 40 neutrons. For each simulated resolution, upper and lower error bounds are calculated using GCI (Equation 7), with an error corridor shown filled in grey: as the simulation is converging, this corridor narrows as the resolution increases.

The best Richardson extrapolated value, (using the finest resolution), is plotted using a green dashed line and has the value 39 neutrons. The simulation with finest resolution, 0.25 μm, gives a neutron yield of 29 with lower and upper bounds calculated using the GCI of 19 and 43 neutrons respectively.

The behaviour of the key fusion metrics BWA density, BWA ion temperature and spherical equivalent burn radius is investigated by plotting their FPA values as functions of resolution as shown in Figure 3 – also plotted is the confinement time, which is the full width at half maximum (FWHM) value of the peak in neutron production rate for each resolution (ie. the FWHM value of each peak in Figure 1a).

Density and ion temperature increase as the resolution becomes finer, with the FPA ion temperature clearly converging to $\sim$240 eV, with less clear convergence seen for the FPA density. Burn radius decreases as the resolution becomes finer, converging to $\sim$2.2 μm. The confinement time appears to be converging to $\sim$ 0.05 ns, but at the finest resolution increases to $\sim$0.1 ns. This can be explained by the splitting of the peak in neutron production rate in Figure 1a. For the simulation at the finest resolution, FPA values are $\langle\rho\rangle_f$=2500 kg m^{-3}, $\langle T_i\rangle_f$=240 eV, $\langle r_b\rangle_f$=2.2 μm and a confinement time $\tau = 0.1$ ns.

IV. CONCLUSIONS

We have successfully simulated the Nevarro target using B2, with spatial convergence approached at a resolution of 0.25 μm. The finest resolution simulation produced a neutron yield of 29 neutrons, with lower and upper bounds of 19 and 43 neutrons respectively; Richardson extrapolation suggests a 'zero resolution' neutron yield of 39 neutrons. The yield occurs in a plasma with an average density 2500 kg m^{-3}, ion temperature 240 eV and a volume equivalent to a sphere of radius 2.2 μm. The predicted neutron yield lies within the error bars of the experiment carried out on the BFG [1]. As the simulations do not contain any physical processes that can produce neutrons other than through thermonuclear fusion reactions, this is indicative that the experimentally observed neutrons are thermonuclear in origin.

[1] G. C. Burdiak, J. W. Skidmore, J. Allison, R. Barker, H. W. Doyle, E. Escauriza, N.-P. L. Niasse, Z. Pešić, T. Ringrose, and N. A. Hawker. 0485: Validate Production of Neutrons from Gas Gun-Driven Targets. Technical report, First Light Fusion Ltd., 2022.

[2] C.W Hirt and B.D Nichols. Volume of fluid (vof) method for the dynamics of free boundaries. *Journal of Computational Physics*, 39(1):201–225, 1981.

[3] Steffen Faik, Anna Tauschwitz, and Igor Iosilevskiy. The equation of state package feos for high energy density matter. *Computer Physics Communications*, 227:117–125, 2018.

[4] R. M. More, K. H. Warren, D. A. Young, and G. B. Zimmerman. A new quotidian equation of state (qeos) for hot dense matter. *Physics of Fluids (1958-1988)*, 31(10):3059–3078, 1988.

[5] L. H. Thomas. The calculation of atomic fields. *Mathematical Proceedings of the Cambridge Philosophical Society*, 23(5):542–548, 1927.

[6] E. Fermi. A statistical method for the determination of some atomic properties and the application of this method to the theory of the periodic systems of elements. *Zeitschrift für Physik*, 48:73, 1928.

[7] Y. T. Lee and R. M. More. An electron conductivity model for dense plasmas. *Physics of Fluids (1958-1988)*, 27(5):1273–1286, 1984.

[8] L. Stanton and M. S. Murillo. Ionic transport in high-energy-density matter. *Phys. Rev. E*, 93:043203, 2016.

[9] E. M. Apfelbaum. The calculations of thermophysical properties of low-temperature gallium plasma. *Physics of Plasmas*, 27:092703, 2020.

[10] G. Hazak, Z. Zinamon, Y. Rosenfeld, and M. W. C. Dharma-wardana. Temperature relaxation in two-temperature states of dense electron-ion systems. *Physical Review E*, 64:066411, 2001.

[11] D. O. Gericke. Kinetic approach to temperature relaxation in dense plasmas. *Journal of Physics: Conference Series*, 11:111, 2005.

[12] J. Vorberger and D. O. Gericke. Comparison of electron-ion energy transfer in dense plasmas obtained from numerical simlulations and quantum kinetic theory. *High energy Density Physics*, 10:1–8, 2014.

[13] D. A. Chapman, J. D. Pecover, N. Chaturvedi, N. Niasse, M. P. Read, D. H. Vassilev, J. P. Chittenden, N. Hawker,

and N. Joiner. A preliminary assessment of the sensitivity of uniaxially driven fusion targets to flux-limited thermal conduction modeling. *Physics of Plasmas*, 28(7):072702, 2021.

[14] H.-S. Bosch and G. M. Hale. Improved formulas for fusion cross-sections and thermal reactivities. *Nuclear Fusion*, 32(4):611, 1992.

[15] D. A. Chapman and M. R. Betney and N. A. Hawker. Determination of the Lawson Number (Fusion Triple Product) for Projectile-Driven ICF from Simulation Output. Technical report, First Light Fusion Ltd., 2022.

[16] Richardson L. F. The approximate arithmetical solution by finite differences of physical problems involving differential equations, with an application to stresses in a masonary dam. *Phil. Trans. Roy. Soc. London*, 210(467):307–357, 1910.

[17] Richardson L. F. and J. A. Gaunt. The deferred approach to the limit. *Phil. Trans. Roy. Soc. London*, 226(643):299–361, 1927.

[18] P. J. Roache. *Verification and Validation in Computational Science and Engineering*. Hermosa Publishers, 1998.

[19] P. J. Roache. Conservatism of the gci in finite volume computations on steady state fluid flow and heat transfer. *ASME Journal of Fluids Engineering*, 125(4):771–772, 2003.